Targeted nanoparticle enhanced proapoptotic peptide as potential therapy for glioblastoma

Lilach Agemy[a,1], Dinorah Friedmann-Morvinski[b,1], Venkata Ramana Kotamraju[a], Lise Roth[a], Kazuki N. Sugahara[c], Olivier M. Girard[d], Robert F. Mattrey[d], Inder M. Verma[b], and Erkki Ruoslahti[a,c,2]

[a]Center for Nanomedicine, Sanford-Burnham Medical Research Institute, University of California, Santa Barbara, CA 93106-9610; [b]Laboratory of Genetics, The Salk Institute for Biological Studies, La Jolla, CA 92037; [c]Cancer Research Center, Sanford-Burnham Medical Research Institute, La Jolla, CA 92037; and [d]Department of Radiology, University of California at San Diego, La Jolla, CA 92103

Edited by Mark Groudine, Fred Hutchinson Cancer Research Center, Seattle, WA, and approved September 16, 2011 (received for review September 9, 2011)

Antiangiogenic therapy can produce transient tumor regression in glioblastoma (GBM), but no prolongation in patient survival has been achieved. We have constructed a nanosystem targeted to tumor vasculature that incorporates three elements: (*i*) a tumor-homing peptide that specifically delivers its payload to the mitochondria of tumor endothelial cells and tumor cells, (*ii*) conjugation of this homing peptide with a proapoptotic peptide that acts on mitochondria, and (*iii*) multivalent presentation on iron oxide nanoparticles, which enhances the proapoptotic activity. The iron oxide component of the nanoparticles enabled imaging of GBM tumors in mice. Systemic treatment of GBM-bearing mice with the nanoparticles eradicated most tumors in one GBM mouse model and significantly delayed tumor development in another. Coinjecting the nanoparticles with a tumor-penetrating peptide further enhanced the therapeutic effect. Both models used have proven completely resistant to other therapies, suggesting clinical potential of our nanosystem.

angiogenesis | apoptosis | tumor targeting | tumor treatment

Tumor blood vessels have become an important therapeutic target. As a tumor grows, the blood vessels grow with it, and this growth primarily takes place through angiogenesis (1, 2). Therefore, inhibiting angiogenesis has become a mainstream therapeutic strategy. The special features of tumor vasculature also enable another strategy, homing-based (synaphic) delivery of drugs (3). Tumor blood vessels express various cell surface and extracellular matrix proteins that normal vessels do not express or do so at much lower levels than tumor vessels (1, 3). These specific vascular markers are readily available to bind circulating ligands, such as peptides and antibodies (4–6). Drugs attached to such ligands become concentrated in tumor tissue, thereby improving efficacy and reducing the exposure of normal tissues (3).

Vascular markers can be explored in an unbiased manner by in vivo screening of phage libraries that display random peptide sequences (7). The CGKRK (Cys-Gly-Lys-Arg-Lys) peptide we used in this study was identified by screening for peptides homing to epidermal tumors in mice (8). Intravenous injected CGKRK recognizes the vessels in most tumors but not those in normal tissues (8).

The α-helical amphipathic peptide $_{D}$[KLAKLAK]$_2$ was originally designed as a synthetic antibacterial peptide that disrupts the bacterial cell membrane but is less toxic to eukaryotic cells (9). However, when internalized into eukaryotic cells, $_{D}$[KLAKLAK]$_2$ disrupts the mitochondrial membrane, which is similar to bacteria membranes, and initiates apoptotic cell death (10). Conjugating $_{D}$[KLAKLAK]$_2$ with homing peptides has produced compounds that specifically accumulate at the homing target, causing cell death (11–15). Here we made a tumor-homing $_{D}$[KLAKLAK]$_2$ compound by conjugating $_{D}$[KLAKLAK]$_2$ to CGKRK. $_{D}$[KLAKLAK]$_2$, however, is a highly toxic compound, even when specifically targeted to tumors (11, 13). Administering toxic drugs in a nanoparticle formulation can reduce toxicity. Examples include paclitaxel–albumin nanoparticles [Abraxane (16)] and doxorubicin liposomes [Doxil (17)], both of which are in clinical use. Other advantages of nanoparticles include the fact that compounds coupled onto their surface are presented in a multivalent fashion, which increases the binding efficiency at the target. Further, multiple functions can be built into a nanoparticle.

Here we assembled a multifunctional theranostic nanoparticle in which the CGKRK peptide provides the targeting function that takes the nanoparticles to tumor vascular cells and into their mitochondria. The nanoparticle uses the mitochondria-targeted $_{D}$[KLAKLAK]$_2$ peptide as the drug and iron oxide as a diagnostic component for MRI. Finally, we combined the nanoparticles with the tumor-penetrating peptide iRGD (18, 19), which enhances the penetration of the nanoparticles into the extravascular tumor tissue. The activity of this nanosystem was tested in one of the most difficult to treat tumors, glioblastoma (GBM). Despite a multimodality treatment approach, which includes surgery, irradiation, and chemotherapy, the median survival in this cancer is only 12 mo (20). Thus, more effective treatments are desperately needed.

Results

CGKRK Peptide Homes to Brain Tumors and Colocalizes with Mitochondria in Cells. We tested a number of previously identified tumor-homing peptides for homing to GBM tumors in mice after an i.v. injection (21, 22). Rhodamine (Rd)-labeled CGKRK peptide (8) strongly accumulated in GBM tumors but not in normal brain or other normal tissues, with the exception of the kidneys, where peptides are excreted (Fig. 1*A* and Fig. S1).

CGKRK is internalized into the target cells and can take a payload with it (8). FAM-CGKRK colocalized with a mitochondrial marker in human umbilical vein endothelial cells (HUVEC) and U87, human GBM cells (Fig. 1*B*). CGKRK bound to mitochondria isolated from mouse liver (Fig. 1*C*). The binding was inhibited by unlabeled CGKRK but not a control peptide with a similar structure (CREKA), demonstrating the specificity of the mitochondria binding. CGKRK-displaying phage showed 80-fold higher binding to the isolated mitochondria than a control phage, further supporting the notion that mitochondria are the primary subcellular target of CGKRK.

Intratumoral Distribution of Iron Oxide Nanoworms Coated with CGKRK$_{D}$(KLAKLAK)$_2$. The mitochondrial localization of CGKRK suggested a way of improving the delivery of a proapoptotic peptide, $_{D}$[KLAKLAK]$_2$, which acts on mitochondria (10). We set up a targeting system that consists of the $_{D}$[KLAKLAK]$_2$ peptide as a drug and CGKRK as a targeting element, coupled to iron oxide nanoparticles, dubbed "nanoworms" (NWs) because of their

Author contributions: L.A., D.F.-M., V.R.K., K.N.S., I.M.V., and E.R. designed research; L.A., D.F.-M., V.R.K., L.R., O.M.G., and E.R. performed research; L.A., D.F.-M., V.R.K., and I.M.V. contributed new reagents/analytic tools; L.A., D.F.-M., V.R.K., K.N.S., O.M.G., R.F.M., I.M.V., and E.R. analyzed data; and L.A., D.F.-M., and E.R. wrote the paper.

Conflict of interest statement: E.R., V.R.K., and K.N.S. are shareholders in CendR Therapeutics Inc., which has rights to some of the technology described in this paper.

This article is a PNAS Direct Submission.

[1]L.A. and D.F.-M. contributed equally to this work.

[2]To whom correspondence should be addressed. E-mail: ruoslahti@sanfordburnham.org.

This article contains supporting information online at www.pnas.org/lookup/suppl/doi:10.1073/pnas.1114518108/-/DCSupplemental.

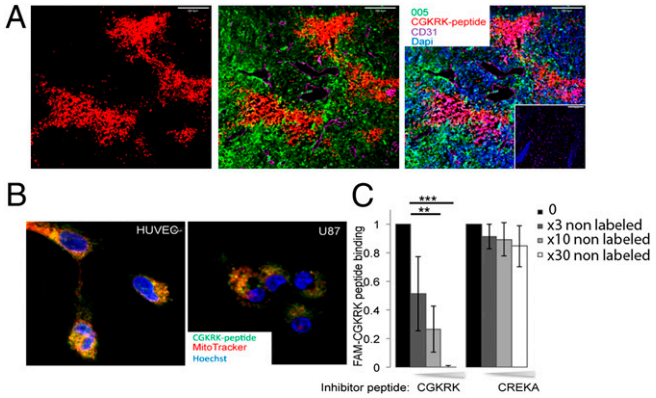

Fig. 1. Homing of CGKRK peptide to GBM tumors and interaction of CGKRK peptide with mitochondria. (*A*) Mice bearing 005 glioma tumors in the right hippocampus were i.v. injected with 200 μg of CGKRK peptide labeled with Rd. After 3 h, the mice were perfused through the heart with PBS, and the tumor and normal brain tissue were collected. *Inset, Right*: Section of normal brain tissue. Red, CGKRK peptide; green, tumor cells; magenta, blood vessels; blue, nuclei. $n = 3$. (Scale bars, 200 μm.) (*B*) Proliferating human endothelial cells (resembling angiogenic endothelial cells) and U87 cells were incubated with FAM-CGKRK peptide (green) and MitoTracker (red) and examined by fluorescent microscopy. Yellow indicates colocalization. (*C*) FAM-CGKRK was incubated with purified mitochondria in the presence of increasing concentrations of either unlabeled CGKRK or an unrelated peptide (CREKA) as a control. Student t test (*C*). Error bars, mean ± SD; n.s., $^{**}P < 0.01$; $^{***}P < 0.001$.

elongated shape and which have been shown to have more effective targeting properties than spherical nanoparticles (23, 24). The two peptides were synthesized as a chimeric peptide, which was covalently linked to the NWs through a 5K-polyethylene glycol (PEG) linker (Fig. 2*A*).

Intravenous injected NWs coated with the chimeric $CGKRK_D[KLAKLAK]_2$ peptide accumulated in tumor vessels in GBM models (mouse 005 transplant tumors and human xenografts from GBM spheres and U87 cells) (Fig. 2*B*). The vessels of the intact brain did not attract $CGKRK_D[KLAKLAK]_2$-NWs (Fig. S2). NWs coated only with CGKRK also accumulated in tumor vessels, whereas $_D(KLAKLAK)_2$-coated NWs did not (Fig. S3*A*). Approximately 80% of tumor vessels were positive for CGKRK-NWs and $CGKRK_D[KLAKLAK]_2$-NWs, whereas only traces of $_D[KLAKLAK]_2$-NWs were found in 4% of the vessels (Fig. S3*B*). The exclusively vascular localization of the NWs is likely due to the inability of the nanoparticles to enter into the tumor tissue, a limitation the free peptide does not have (Fig. 1*A*). No fluorescence from the various NW formulations was observed in normal tissues of the tumor-bearing mice, with the exception of the liver and the spleen, which take up all nanoparticles nonselectively (Fig. S2). When the fluorophore was on the $_D[KLAKLAK]_2$ peptide, the kidneys were also positive, presumably because that is where this nondegradable peptide, having been separated from the NWs, is excreted. MRI of 005 tumors after i.v. injection of $CGKRK_D[KLAKLAK]_2$-NWs showed hypointense signals throughout the tumor due to the presence of the NWs (Fig. 2*C*). This result confirms the tumor localization of the NWs and suggests a possible utility of this reagent in GBM imaging.

$CGKRK_D[KLAKLAK]_2$-NWs Target Mitochondria and Induce Apoptosis. We next tested CGKRK in nanoparticle delivery to mitochondria in cultured cells. $CGKRK_D[KLAKLAK]_2$-NWs and CGKRK-NWs were taken up into HUVEC cells and colocalized with mitochondria, whereas $_D[KLAKLAK]_2$-NWs produced only a minor signal at mitochondria (Fig. 3*A*). Thus, CGKRK can deliver inorganic nanoparticles to mitochondria.

The $CGKRK_D[KLAKLAK]_2$-NWs were cytotoxic to cultured tumor cells, whereas NWs coated with either peptide alone were inactive in this regard. The nanoparticle-coupled peptide was

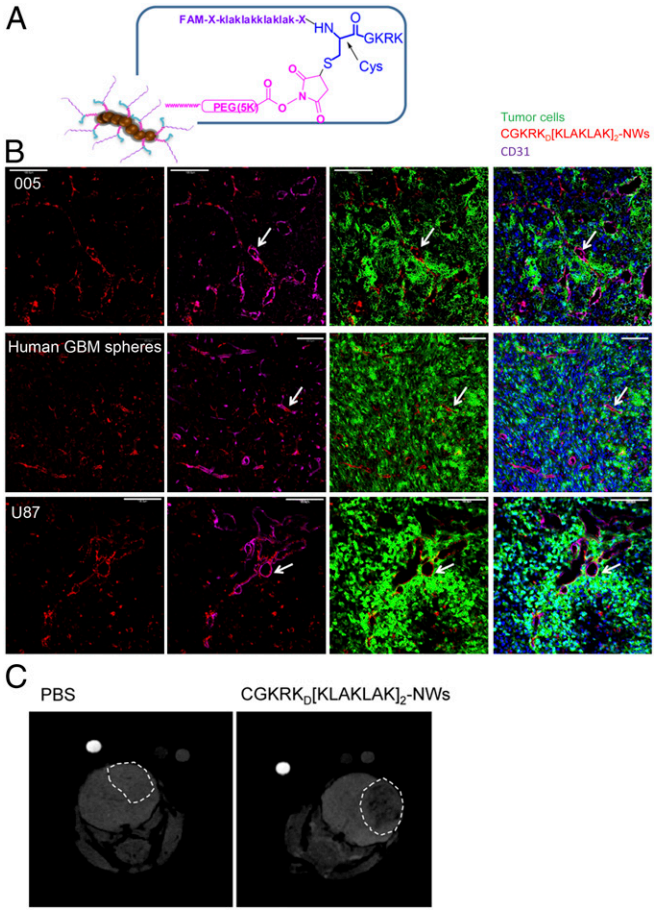

Fig. 2. Homing of $CGKRK_D[KLAKLAK]_2$ NWs to GBM tumors. (*A*) General design of theranostic NWs. A chimeric peptide consisting of a tumor-homing peptide (CGKRK) and a proapoptotic peptide ($_D[KLAKLAK]_2$) is covalently coupled to iron oxide nanoparticles (NWs; length 80–100 nm, width 30 nm); FAM, carboxyfluorescein. (*B*) Iron oxide NWs coated with Rd-labeled $CGKRK_D[KLAKLAK]_2$ peptide through a 5KPEG linker were i.v. injected (5 mg iron per kg body weight) into mice bearing either 005 tumors or xenograft tumors generated with human GBM spheres or U87 cells. The tumor cells were injected into the right hippocampus. Five to six hours after the injection, the mice were perfused through the heart with PBS, and the organs were collected. Tumor sections were stained and examined by confocal microscopy. Red, $CGKRK_D[KLAKLAK]_2$-coated particles; green, tumor cells (both the human GBM spheres and U87 cells expressed green fluorescent protein); magenta, blood vessels stained with anti-CD31; blue, nuclei stained with DAPI. Arrows show representative blood vessels that accumulate $CGKRK_D[KLAKLAK]_2$-NW for each tumor model. (Scale bars, 100 μm.) (*C*) T2*-weighted MRI. Rd-labeled $CGKRK_D[KLAKLAK]_2$-NWs were i.v. injected into tumor-bearing mice. Grayscale images of axial planes through the tumors are shown. Gadolinium (Gd) and Feridex (Fe) were used as reference standards. $n = 3$–4.

hundreds of times more active than the free peptide on a molar basis (Fig. 3*B*). Previous reports have shown that $_D[KLAKLAK]_2$-homing peptide conjugates cause cell death via apoptosis (10), although necrosis may also be a factor (11). Treatment of cultured cells with $[KLAKLAK]_2$-NWs and $CGKRK_D[KLAKLAK]_2$-NWs induced annexin V staining in activated HUVECs (approximately 60% after 48 h) and T3 GBM cells (approximately 35% after 72 h) (Fig. 3*C* and Fig. S4 *A* and *B*). CREKA-NWs and CGKRK-NWs had no significant effect. However, when the nanoparticle-treated cells were washed after 30 min of incubation, only $CGKRK_D[KLAKLAK]_2$-NWs induced significant apoptosis, emphasizing the importance of the targeting peptide (Fig. 3*D* and Fig. S4*C*). $CGKRK_D[KLAKLAK]_2$-NWs also induced caspase-3 cleavage (Fig. 3 *E* and *F*), further supporting apoptosis as the cell death mechanism.

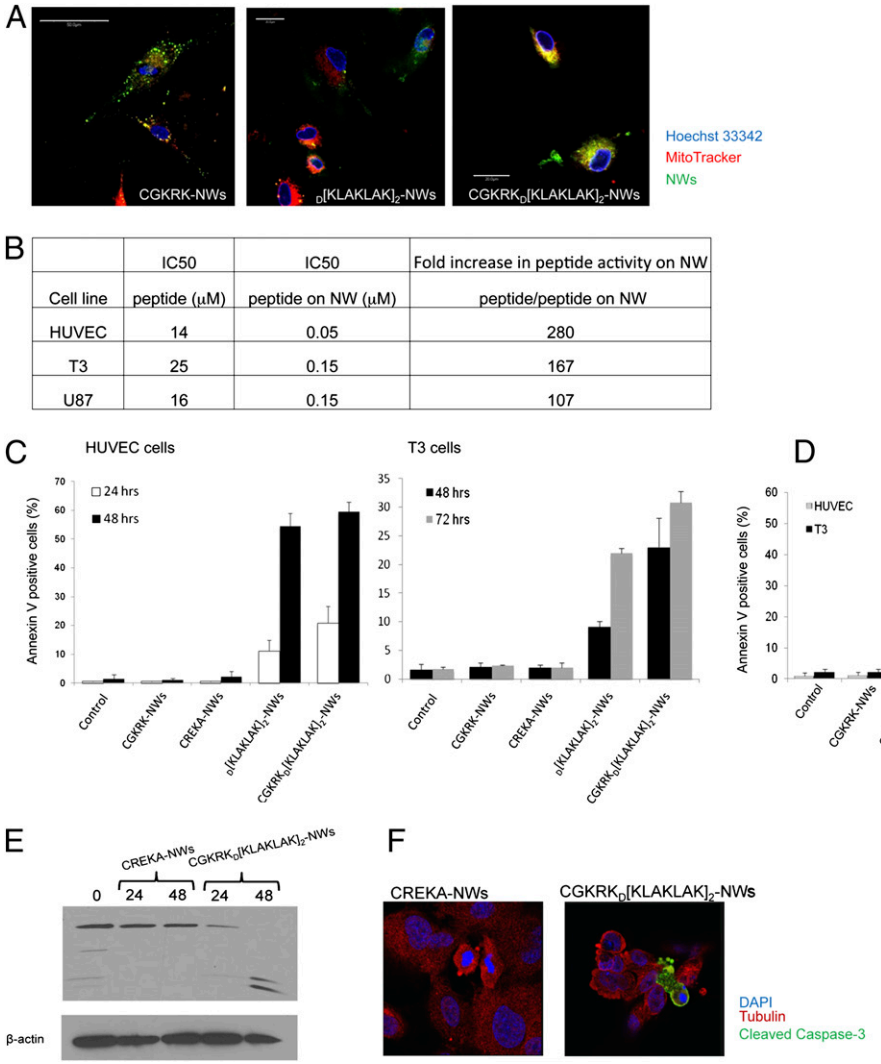

Cell line	IC50 peptide (μM)	IC50 peptide on NW (μM)	Fold increase in peptide activity on NW peptide/peptide on NW
HUVEC	14	0.05	280
T3	25	0.15	167
U87	16	0.15	107

Fig. 3. $_D$[KLAKLAK]$_2$CGKRK-NW conjugates internalize into activated endothelial cells, colocalize with mitochondria, and induce cell death by apoptosis. (*A*) Confocal microscopic images of live HUVEC incubated for 2 h at 37 °C in the presence of fluorescein (FAM)-labeled NWs (green) and a marker for mitochondria (MitoTracker; red) for 15 min before the imaging. DNA was counterstained with Hoechst 33342 (blue). (Scale bars, 20 μm.) (*B*) FAM-CGKRK$_D$[KLAKLAK]$_2$ peptide was coupled onto the NWs via a reducible 5KPEG linker. The linker was cleaved from the NWs using DTT, and the amount of peptide present on the NWs was determined by fluorescence measurements in solution (to circumvent quenching on the NW surface) and used to calculate IC$_{50}$. (*C* and *D*) HUVEC and T3 cells were left untreated (Control) or treated with a concentration of 10 μg/mL of NWs coated with either a control peptide (CREKA), $_D$[KLAKLAK]$_2$, or CGKRK$_D$[KLAKLAK]$_2$ for 24, 48, and 72 h (*C*), or the particles were washed away after 30 min and the incubation continued for 72 h (*D*). The cells were stained with annexin and analyzed by flow cytometry. The total percentage of annexin-positive cells (apoptotic and dead cells) is indicated. (*E*) Whole cell extracts (HUVEC) from the experiment in *C* were prepared and analyzed by immunoblotting using antibodies against cleaved caspase-3 and β-actin as loading control. (*F*) Confocal microscopy images of HUVEC treated with the indicated NWs and stained for cleaved caspase-3 (green), tubulin (red), and nuclei (blue). (Scale bars, 50 μm.)

CGKRK$_D$[KLAKLAK]$_2$-NWs significantly reduced the ability of HUVEC to form tube-like structures in a Matrigel angiogenesis assay, whereas CGKRK-NWs were inactive (Fig. S5*A*). To assess in vivo effects, mice bearing bFGF-impregnated Matrigel plugs were i.v. injected with CGKRK$_D$[KLAKLAK]$_2$-NWs or PBS every other day for 2 wk. After 14 d the mice were perfused with cy5-labeled isolectin, and the plugs were excised. Imaging of the plugs by confocal microscopy showed a significant decrease in blood vessels in the NW-treated mice (Fig. S5*B*).

Therapeutic Efficacy of NW in GBM. Given that CGKRK$_D$[KLAKLAK]$_2$ coated onto NWs was more effective in inducing cell death than soluble CGKRK$_D$[KLAKLAK]$_2$, we hypothesized that the NW-based approach might be more effective and/or less toxic than the monovalent homing peptide–[KLAKLAK]$_2$ conjugates used previously (10, 11). We tested this possibility in mouse GBM models that closely resemble human GBMs in their aggressiveness and in the diffuse spreading of the tumor cells into the normal brain tissue (21). Like most human GBMs, the tumors in these mouse models are highly angiogenic, and the vasculature is considered a promising therapeutic target (25). Thus, our nanoparticles, which target tumor blood vessels, seemed an appropriate candidate to test in GBM.

In one model, a single lentiviral vector expressing H-RasV12 oncogene and an shRNA targeting p53 is injected into the hippocampus of mice (22). The mice invariably develop GBMs that have a highly predictable course of tumorigenesis and are lethal to the mice within 2–3 mo after injection. These mice were treated with systemic injections every other day over 3 wk, starting 3 wk after tumor induction. Separate analysis by microscopy showed that the tumors were 0.8 to1.0 mm^3 at this stage. In the experimental glioma treatment literature, tumors of this size are considered well

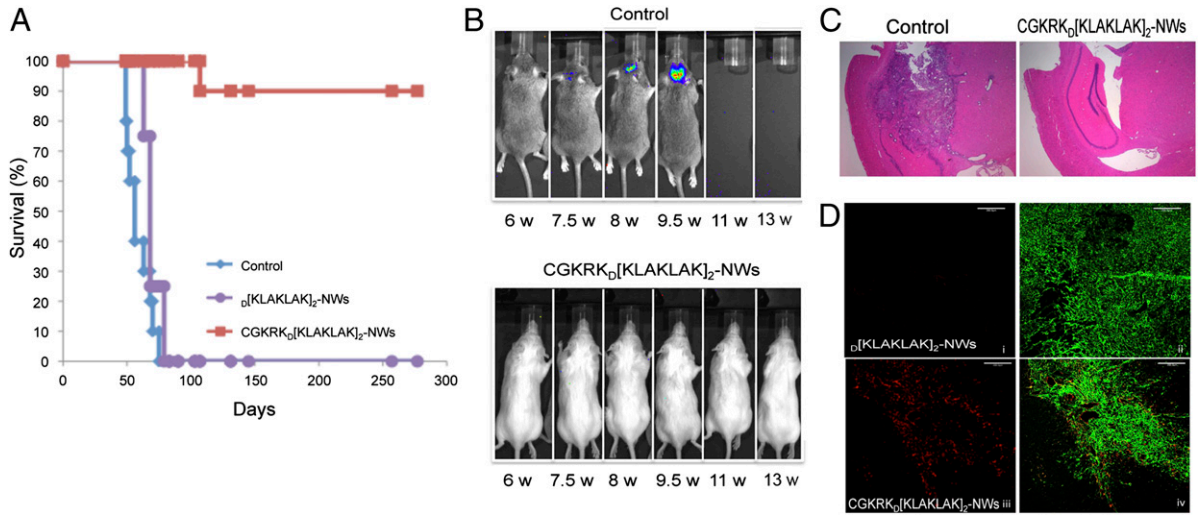

Fig. 4. CGKRK$_D$[KLAKLAK]$_2$-NW treatment of tumors induced by lentiviral injection. Mice bearing lentiviral (H-RasV12-shp53) induced brain tumors in the right hippocampus were i.v. injected with NW coated with peptides. The particles were administered every other day for 18 d, starting 3 wk after viral injection. (*A*) Survival curve of the nontreated and treated mice (n = 8–10 per group). (*B*) Mice were monitored for luciferase signal using the IVIS system (the lentiviral vector contains the luciferase reporter); one representative mouse from each of the indicated groups is shown. (*C*) H&E staining showing the lentiviral injection site in a representative control mouse and a mouse treated with CGKRK $_D$[KLAKLAK]$_2$-NWs at the end of treatment. (*D*) Confocal microscopy images of brain sections from a representative mouse at the end of the treatment with $_D$[KLAKLAK]$_2$-NWs (*Di* and *Dii*) and from a CGKRK $_D$[KLAKLAK]$_2$-NW–treated mouse that contained a small residual tumor (*Diii* and *Div*) (red); green, tumor cells. (Scale bars, 200 μm.)

established (e.g., ref. 26). As expected, mice that received the vehicle only (PBS) all succumbed to the disease within 8–9 wk, and $_D$[KLAKLAK]$_2$-NWs provided no survival benefit. In sharp contrast, systemic CGKRK$_D$[KLAKLAK]$_2$-NWs cured all but 1 of 10 mice (Fig. 4*A*). We monitored the tumor mice by luciferase imaging (the lentiviral vector contains the luciferase reporter). The imaging was not strong enough to detect the 1-mm^3 tumors at 6 wk when the treatment was stopped, but positive signals were seen in the control-treated mice at ≈7.5 wk after injection of the virus. No tumors were detected by imaging in the mice treated with CGKRK$_D$[KLAKLAK]$_2$-NWs (Fig. 4*B*). Histological analysis showed no detectable tumor tissue in mice treated with CGKRK$_D$[KLAKLAK]$_2$-NWs (Fig. 4*C*). CGKRK$_D$[KLAKLAK]$_2$-NW–treated tumors, when present, were small and contained abundant NWs in the blood vessels (Fig. 4*D*), whereas the mice treated with the nontargeted $_D$[KLAKLAK]$_2$-NW had large tumors with no NWs.

Toxicology analyses indicated some liver toxicity (nanoparticles nonspecifically accumulate in the liver) judging from a moderate elevation in the serum level of the liver enzyme L-alanine-2-oxoglutarate aminotransferase (Fig. S6*A*). The values normalized within 2 wk after the treatment was discontinued. The particles were not immunogenic, as determined by ELISA (Fig. S6*B*). An IL-6 assay indicated low-level macrophage activation in CGKRK$_D$[KLAKLAK]$_2$-NWs–treated mice (Fig. S6*C*). No evidence of kidney damage was detected in H&E-stained sections (Fig. S6*D*). These modest toxicities are in contrast with the severe toxicity of the monovalent $_D$[KLAKLAK]$_2$ conjugates observed previously (e.g., refs. 11 and 13).

We also tested the NW treatment in a transplantable model that uses a GBM cell line (005) established from a lentivirally induced tumor (21). Mice transplanted with 005 tumor cells usually die 4–6 wk after inoculation. The tumors display invasive properties similar to the lentiviral model and human GBM. CGKRK$_D$[KLAKLAK]$_2$-NW treatment increased median survival from 32 to 52 d (Fig. 5*A*). Continuous treatment did not provide further survival benefit (Fig. 5*A*).

Confocal microscopy at the end of treatment showed that vascular structures in the 005 tumors were often filled with CGKRK$_D$(KLAKLAK)$_2$-NWs (Fig. 5*B*), and lectin perfusion revealed an almost complete absence of patent blood vessels, indicating destruction of the vessels by the NWs (Fig. 5*C*). Clusters of TUNEL staining-positive cells in the CGKRK$_D$(KLAKLAK)$_2$-NW–treated but not in control-treated tumors also indicated vascular destruction (Fig. S7).

We also tested the CGKRK$_D$(KLAKLAK)$_2$-NW treatment in a well-established human xenograft model, tumors induced with orthotopic injection of U87 human GBM cells. The treatment also prolonged survival in this model (Fig. S8).

Combining CGKRK$_D$(KLAKLAK)$_2$-NW with iRGD Enhances Nanoparticle Penetration and Therapeutic Efficacy. A tumor-penetrating peptide, iRGD (sequence: CRGDKGPDC), enhances tumor penetration of iRGD-bound and coadministered compounds (18, 19). Combining the CGKRK$_D$[KLAKLAK]$_2$-NWs with iRGD in the 005 tumor model, in which the NW treatment was only partially successful, substantially prolonged survival (Fig. 6*A*). Confocal microscopy analysis showed that the NWs coinjected with iRGD had spread into the extravascular tumor tissue, whereas NWs coinjected with CRGDC mainly accumulated in tumor vessels (Fig. 6*B*). This conclusion was confirmed by quantifying the nanoparticle signal outside the blood vessels (Table S1).

Discussion

Our nanoparticle system allows an impressive degree of control in GBM mouse models that closely resemble the pathobiology of human GBMs: we were able to cure most of the GBM mice in one model and greatly prolong the lifespan in another.

One key to the efficacy of the system is the CGKRK, tumor-homing peptide, which provides the targeting function to the system. It specifically delivers its payload not only to the tumor vasculature but also to a specific subcellular location, the mitochondria. We made use of this unique ability of CGKRK to reach the mitochondria by using the amphiphilic proapoptotic peptide $_D$[KLAKLAK]$_2$ as the payload. $_D$[KLAKLAK]$_2$ has been shown to act on mitochondria, the target of CGKRK (10), and several reports have described the antitumor activities of $_D$[KLAKLAK]$_2$ (and some other peptides with similar activities), when selectively delivered to a target tissue (11–15, 27–29). The main limitation of these treatments has been that the $_D$[KLAKLAK]$_2$ peptide is highly toxic at the doses required for tumor treatment even with specific targeting. The presumed reason is kidney toxicity of the nondegradable D-conformer (13). The vastly enhanced activity of the multimeric CGKRK$_D$[KLA-

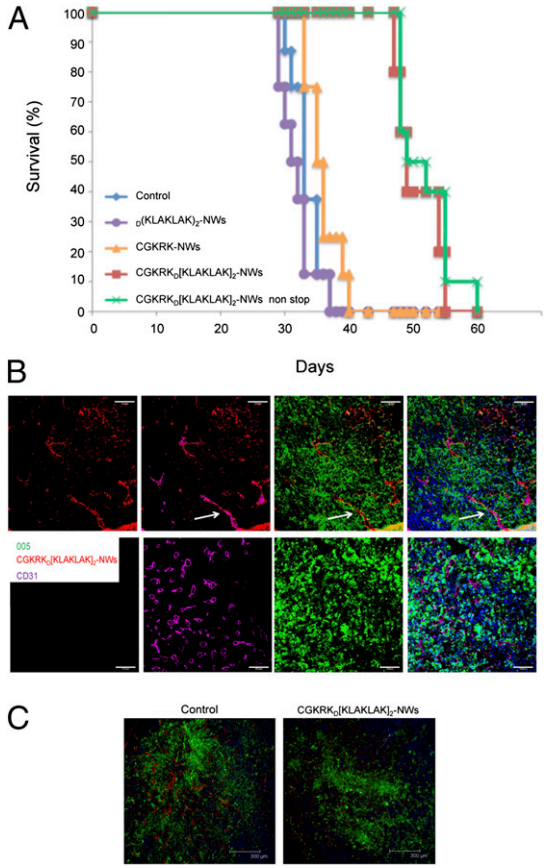

Fig. 5. Treatment of transplanted GBM tumors with CGKRK$_D$[KLAKLAK]$_2$-NWs. Tumors were developed by transplanting 3×10^5 005 cells into the right hippocampus of NOD-SCID mice. Ten days after tumor cell transplantation, the mice were i.v. injected with NWs. The NWs (5 mg iron/kg) were administered every other day for 3 wk or administered nonstop for the same period (n = 8 per group). (*A*) Survival curve of the treated mice. (*B*) Brain sections at the end of the treatment were stained: magenta, anti-CD31; red, CGKRK$_D$[KLAKLAK]$_2$-NWs or $_D$[KLAKLAK]$_2$-NWs; green, tumor cell; blue, DAPI. Arrows show representative blood vessels that accumulate CGKRK$_D$[KLAKLAK]$_2$-NW in the tumor. (Scale bars, 200 mm.) (*C*) Lectin perfusion of tumor mice at the end of the treatment. Vessels were stained by perfusion of biotinylated *Lycopersicon esculentum* lectin and visualized by confocal microscopy using anti-biotin. Green, tumor cells; red, perfused, lectin-labeled blood vessels; blue, nuclei (DAPI).

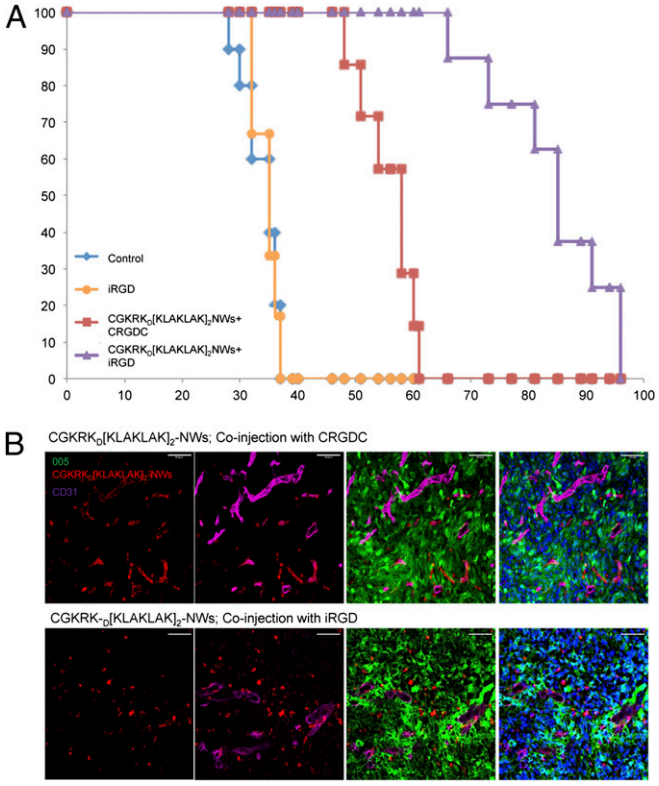

Fig. 6. Enhanced antitumor effect of CGKRK$_D$[KLAKLAK]$_2$-NWs coinjected with iRGD. (*A*) Mice bearing orthotopic 005 tumors implanted 10 d earlier received every other day for 3 wk i.v. injections of either CGKRK$_D$[KLAKLAK]$_2$-NWs (5 mg iron/kg) or CGKRK$_D$[KLAKLAK]$_2$-NWs (5 mg/kg) mixed with 4 mmol/kg of iRGD or PBS. Survival curves are shown (n = 8–10 per group). (*B*) Mice bearing orthotopic 005 tumors were i.v. injected with CGKRK$_D$[KLAKLAK]$_2$-NW (5 mg iron/kg) in combination with 4 mmol/kg of either nonlabeled CRGDC (*Upper*) or iRGD (*Lower*) peptide. The tumors and tissues were collected 5–6 h later and analyzed by confocal microscopy. Red, CGKRK$_D$[KLAKLAK]$_2$-NWs; magenta, blood vessels; green, tumor cell; blue, DAPI. (Scale bars, 50 mm.)

KLAK]$_2$ on NWs allowed us to lower the $_D$[KLAKLAK]$_2$ dose 100-fold, which largely corrected the toxicity problem. Multivalent display of the $_D$[KLAKLAK]$_2$ on nanoparticles has been reported to enhance in vitro internalization of the nanoparticles into cells (29). In our hands, NW-bound $_D$[KLAKLAK]$_2$ was also highly cytotoxic, but adding the CGKRK homing peptide greatly increased the activity against tumor cells and activated endothelial cells. In agreement with these in vitro results, the CGKRK$_D$[KLAKLAK]$_2$-NWs selectively homed to the tumors and inhibited tumor growth in vivo. In contrast, NWs displaying the proapoptotic peptide without CGKRK showed no tumor homing and no effect on tumor growth. Thus, efficient targeting is likely the main contributor to the selective antitumor activity.

GBMs are generally highly vascularized tumors, and VEGF is produced at high levels by the tumor cells (25, 30). Therefore, antiangiogenic therapy has been considered a promising strategy for these tumors (30). However, antiangiogenic agents such as the VEGF inhibitor bevacizumab have demonstrated only a marginal efficacy in clinical GBM (31), and the anti-VEGF receptor inhibitor AG28262 has been found to give no significant survival benefit in the H-RasV12-shp53 lentivirus-induced GBM model we used in this study (22). Transdifferentiation of tumor cells into endothelial cells has been observed in GBMs (22, 32, 33), and antiangiogenic therapy has been shown to increase the rate of the transdifferentation. Because the transdifferentiation cells do not need VEGF, the transdifferentiation is the likely explanation for the resistance of GBM to anti-VEGF therapies (22). Our therapeutic approach is independent of the VEGF–VEGFR interaction, and unlike the existing antiangiogenic therapies, CGKRK$_D$[KLAKLAK]$_2$-NWs showed significant efficacy in both lentiviral-induced and 005 transplanted models. These treatment results, and the robust in vitro cytotoxicity of CGKRK$_D$[KLAKLAK]$_2$-NWs to GBM-derived endothelial cells (T3 cells) we observed, suggest that the NWs target both the ordinary and transdifferentiated vessels.

Despite the obvious efficacy of CGKRK$_D$[KLAKLAK]$_2$-NWs, the 005 GBM mice eventually succumbed to the disease. A surprising finding was that these treated tumors continued to grow even though they were essentially devoid of functional blood vessels. The formation of fluid-conducting channels lined by tumor cells, vasculogenic mimicry, could produce vessels that are not recognized by the lectin we used to detect patent blood vessels, possibly explaining this paradox (34, 35).

Combining CGKRK$_D$[KLAKLAK]$_2$-NWs with the tumor-penetrating peptide iRGD further increased the survival of the 005 GBM mice. This peptide promotes the penetration of coadministered drugs and nanoparticles into extravascular tumor tissue (18),

which was also observed with the current $CGKRK_D[KLAKLAK]_2$-NWs system. The likely reason for the improved survival of the mice treated with the combination is that iRGD allows the NWs to reach the tumor cells, not just the tumor vessels.

In summary, we describe a nanosystem that targets GBM tumors that provides both effective therapeutic activity and a diagnostic function and is augmented by the use of iRGD. The efficacy and low toxicity we observed in these preclinical studies encourages further development of the system toward clinical application in GBM, where new therapies are desperately needed, and potentially in other cancers as well.

Methods

Peptide Synthesis. Peptides were synthesized by solid phase methods (23).

Flow Cytometry. Cells were harvested and stained using the annexin V-phycoerythrin apoptosis detection kit (BD Pharmingen) and analyzed on a BD LSR II flow cytometer (Becton Dickinson).

In Vivo Peptide Homing In vivo peptide homing was tested as previously described (23).

In Vivo NW Injections. Mice bearing orthotopic GBM tumors were injected into the tail vein with NWs (5 mg of iron per kg body weight). In homing experiments, the mice were killed 5–6 h after the injection by cardiac perfusion with PBS under anesthesia, and organs were dissected and analyzed for NWs. In tumor treatment experiments, tumor mice were i.v. injected with NWs in 150 μL PBS, or PBS as a control every other day for 3 wk. Mice with 005 tumors were also i.v. injected with $CGKRK_D[KLAKLAK]_2$-NW (5 mg iron/kg) in combination with 4 mmol/kg of either the tumor-penetrating peptide iRGD or CRGDC as a control. At the end of treatment two mice per group were killed, and the rest of the mice were monitored until the animal facility staff determined that a mouse's symptoms required killing.

Histology and Immunohistology. Tissue sections were processed as previously described (23).

The following methods are described in detail in *SI Methods*: cell lines and tumors; magnetic resonance imaging; preparation of NWs; biophotonic tumor imaging; isolation of mitochondria and peptide/phage binding; cell proliferation assay and imaging; and immunoblot analysis of NW-bound proteins.

Statistical Analysis. Data were analyzed by two-tailed Student's unpaired *t* test. *P* values of <0.05 were considered statistically significant.

ACKNOWLEDGMENTS. We thank Drs. Michael J. Sailor and Ji-Ho Park for advice in the synthesis of iron oxide nanoparticles, Dr. Eva Engvall for comments on the manuscript, Dr. Khatereh Motamedchaboki for protein identification, Jacqueline Corbeil for help with magnetic resonance imaging, and Gabriela Estepa for technical help. This work was supported by National Cancer Institute Grants CA152327 and CA124427 (to E.R.), Cancer Center Support Grant CA30199 (to the Sanford-Burnham Medical Research Institute), National Institute of Allergy and Infectious Diseases Grant R37AI048034, the Leducq Foundation, the Merieux Foundation, Ipsen/Biomeasure, and H.N. and Frances C. Berger Foundation grants (to I.M.V.). D.F.-M. was supported by the European Molecular Biology Organization. I.M.V. is an American Cancer Society Professor of Molecular Biology and holds the Irwin and Joan Jacobs Chair in Exemplary Life Sciences.

1. Hanahan D, Folkman J (1996) Patterns and emerging mechanisms of the angiogenic switch during tumorigenesis. *Cell* 86:353–364.
2. Ferrara N, Alitalo K (1999) Clinical applications of angiogenic growth factors and their inhibitors. *Nat Med* 5:1359–1364.
3. Ruoslahti E, Bhatia SN, Sailor MJ (2010) Targeting of drugs and nanoparticles to tumors. *J Cell Biol* 188:759–768.
4. Allen TM, Cullis PR (2004) Drug delivery systems: Entering the mainstream. *Science* 303:1818–1822.
5. Jain RK, Gerlowski LE (1986) Extravascular transport in normal and tumor tissues. *Crit Rev Oncol Hematol* 5:115–170.
6. Ruoslahti E (2002) Specialization of tumour vasculature. *Nat Rev Cancer* 2:83–90.
7. Pasqualini R, Ruoslahti E (1996) Organ targeting in vivo using phage display peptide libraries. *Nature* 380:364–366.
8. Hoffman JA, et al. (2003) Progressive vascular changes in a transgenic mouse model of squamous cell carcinoma. *Cancer Cell* 4:383–391.
9. Javadpour MM, et al. (1996) De novo antimicrobial peptides with low mammalian cell toxicity. *J Med Chem* 39:3107–3113.
10. Ellerby HM, et al. (1999) Anti-cancer activity of targeted pro-apoptotic peptides. *Nat Med* 5:1032–1038.
11. Arap W, et al. (2002) Targeting the prostate for destruction through a vascular address. *Proc Natl Acad Sci USA* 99:1527–1531.
12. Fantin VR, et al. (2005) A bifunctional targeted peptide that blocks HER-2 tyrosine kinase and disables mitochondrial function in HER-2-positive carcinoma cells. *Cancer Res* 65:6891–6900.
13. Karjalainen K, et al. (2011) Targeting neuropilin-1 in human leukemia and lymphoma. *Blood* 117:920–927.
14. Mai JC, Mi Z, Kim SH, Ng B, Robbins PD (2001) A proapoptotic peptide for the treatment of solid tumors. *Cancer Res* 61:7709–7712.
15. Rege K, Patel SJ, Megeed Z, Yarmush ML (2007) Amphipathic peptide-based fusion peptides and immunoconjugates for the targeted ablation of prostate cancer cells. *Cancer Res* 67:6368–6375.
16. Gradishar WJ, et al. (2005) Phase III trial of nanoparticle albumin-bound paclitaxel compared with polyethylated castor oil-based paclitaxel in women with breast cancer. *J Clin Oncol* 23:7794–7803.
17. Haley B, Frenkel E (2008) Nanoparticles for drug delivery in cancer treatment. *Urol Oncol* 26:57–64.
18. Sugahara KN, et al. (2010) Coadministration of a tumor-penetrating peptide enhances the efficacy of cancer drugs. *Science* 328:1031–1035.
19. Sugahara KN, et al. (2009) Tissue-penetrating delivery of compounds and nanoparticles into tumors. *Cancer Cell* 16:510–520.
20. Wen PY, Kesari S (2008) Malignant gliomas in adults. *N Engl J Med* 359:492–507.
21. Marumoto T, et al. (2009) Development of a novel mouse glioma model using lentiviral vectors. *Nat Med* 15:110–116.
22. Soda Y, et al. (2011) Transdifferentiation of glioblastoma cells into vascular endothelial cells. *Proc Natl Acad Sci USA* 108:4274–4280.
23. Agemy L, et al. (2010) Nanoparticle-induced vascular blockade in human prostate cancer. *Blood* 116:2847–2856.
24. Park JH, et al. (2009) Systematic surface engineering of magnetic nanoworms for in vivo tumor targeting. *Small* 5:694–700.
25. Chi AS, Sorensen AG, Jain RK, Batchelor TT (2009) Angiogenesis as a therapeutic target in malignant gliomas. *Oncologist* 14:621–636.
26. Kunkel P, et al. (2001) Inhibition of glioma angiogenesis and growth in vivo by systemic treatment with a monoclonal antibody against vascular endothelial growth factor receptor-2. *Cancer Res* 61:6624–6628.
27. Marks AJ, et al. (2005) Selective apoptotic killing of malignant hemopoietic cells by antibody-targeted delivery of an amphipathic peptide. *Cancer Res* 65:2373–2377.
28. Ko YT, Falcao C, Torchilin VP (2009) Cationic liposomes loaded with proapoptotic peptide D-(KLAKLAK)(2) and Bcl-2 antisense oligodeoxynucleotide G3139 for enhanced anticancer therapy. *Mol Pharm* 6:971–977.
29. Standley SM, et al. (2010) Induction of cancer cell death by self-assembling nanostructures incorporating a cytotoxic peptide. *Cancer Res* 70:3020–3026.
30. Jain RK, et al. (2007) Angiogenesis in brain tumours. *Nat Rev Neurosci* 8:610–622.
31. Vredenburgh JJ, et al. (2007) Phase II trial of bevacizumab and irinotecan in recurrent malignant glioma. *Clin Cancer Res* 13:1253–1259.
32. Ricci-Vitiani L, et al. (2010) Tumour vascularization via endothelial differentiation of glioblastoma stem-like cells. *Nature* 468:824–828.
33. Wang R, et al. (2010) Glioblastoma stem-like cells give rise to tumour endothelium. *Nature* 468:829–833.
34. Hendrix MJ, Seftor EA, Hess AR, Seftor RE (2003) Vasculogenic mimicry and tumour-cell plasticity: lessons from melanoma. *Nat Rev Cancer* 3:411–421.
35. Yue WY, Chen ZP (2005) Does vasculogenic mimicry exist in astrocytoma? *J Histochem Cytochem* 53:997–1002.